

SUPPLEMENTARY FIGURE LEGENDS

Supplemental Fig. S1. Color-coded firing rate maps are shown for the remainder of CA3 and CA1 place cells from Day 4 sessions for the example rat from the single location training group shown in Fig. 3D. Each map is shown scaled to the maximum firing rate across all sessions (top row for each cell), and the same maps are shown scaled to the maximum firing rate within each session (bottom row for each cell). The maximum firing rates for each session are indicated with white numbers on the map. In the color scale, red symbolizes the peak rate, blue represents no firing, and white pixels indicate areas that were not visited during the session.

Supplemental Fig. S2. Color-coded firing rate maps from the morph day are shown for the remainder of CA3 (page 1) and CA1 (page 2) place cells for the example rat from the *single location* training group shown in Fig. 5A, B. Presentation and color scaling of maps is as described for Supplemental Fig. S1.

Supplemental Fig. S3. Mean (\pm s.e.m.) spatial correlation (A, B for CA3 and CA1, respectively) and rate overlap (C, D for CA3 and CA1, respectively) measures are shown for morph day session pairs for the *single location* training group. Open circles indicate expected values (see Materials and Methods). For opposite shapes, changes in rate overlap combined with no detectable differences in spatial correlations indicate that effects in the *single location* training group primarily involved changes in firing rates but not place field locations.

Supplemental Fig. S4. A, B, For CA3 (A) and CA1 (B) place cells, 28 and 38 fields, respectively, surpassed the 2 Hz in-field mean firing rate threshold used for this analysis. 11 of the fields in CA3 and 8 of the fields in CA1 exhibited firing rate changes across successively different shapes that were significantly fit by a sigmoid function. Transitions for fields with significant sigmoid curve fits did not all occur at a coherent point but were instead distributed across the entire extent of progressive shape changes.

Supplemental Fig. S5. Color-coded CA3 population vector cross-correlation matrices (color scale and axes as in Fig. 4) for morph day session pairs in the *single location* training group. The cross-correlation matrices between the initial circle session and all other shapes are shown, and a clear central peak is seen for all shape pairs. The lowest correlation value was

observed between the square and the circle, and correlations increased gradually as the shapes became more similar.

Supplemental Fig. S6. Color-coded firing rate maps from Day 4 are shown for the remainder of CA3 and CA1 place cells for the example rat from the *two location* training group shown in Fig. 8D. Maps are shown scaled to the maximum rate across all sessions (top row for each cell) and to their own maximum rate (bottom row for each cell). Color scale is as described for Supplemental Fig. S1.

Supplemental Fig. S7. Color-coded firing rate maps from the morph sequence are shown for the remainder of CA3 and CA1 place cells for the example rat from the *two location* training group shown in Fig. 10A, B. Maps are shown scaled to the maximum rate across all sessions (top row for each cell) and to their own maximum rate (bottom row for each cell). Color scale is as described for Supplemental Fig. S1.

Supplemental Fig. S8. Mean (\pm s.e.m.) spatial correlation (**A** for CA3 and **B** for CA1) and rate overlap (**C** for CA3 and **D** for CA1) measures are shown for morph day session pairs for the *double location* training group. Open circles indicate expected values (see Materials and Methods). Midway through the sequence, low values for dissimilar shape pairs change abruptly to high values for similar shape pairs.

Supplemental Fig. S9. For CA3 (**A**) and CA1 (**B**), 51 and 21 fields, respectively, in the *two location* training group exhibited in-field mean firing rates greater than 2 Hz in at least one of the shapes and were included in this analysis. 34 fields in CA3 and 9 fields in CA1 exhibited firing rate changes across successively different shapes that were significantly fit by a sigmoid function. Almost all of the sigmoid fits showed a transition at the midpoint of the sequence of intermediate shapes.

Supplemental Fig. S10. Color-coded population vector cross-correlation matrices (color code and axes as described in Fig. 4) for CA3 rate maps on the morph day in the *two location* training group for the initial circle paired with the sequence of shapes shown above. Strong peaks in the center of the matrix can be seen for the circle-circle cross-correlations. Faint peaks of near zero magnitude are seen in the cross-correlation matrices for the circle-square pair and for the circle paired with the two most square-like intermediate shapes. At the central transition point in the morph sequence, the clear peak in the center of the cross-

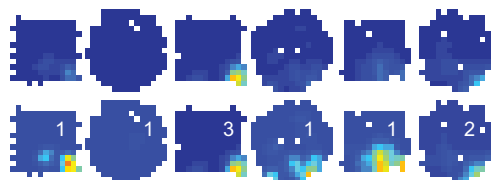
correlation matrix reappears and is observed for the cross-correlations between the circle and the circle-like intermediate shapes.

Supplemental Fig. S1

Single location training, Day 4, Rat 3

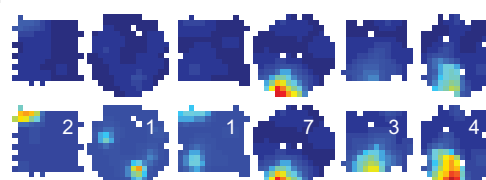
CA3

Cell 6

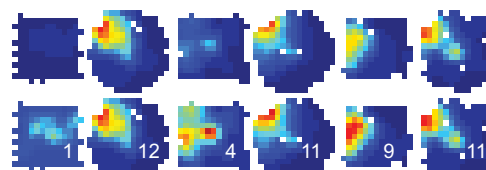


CA1

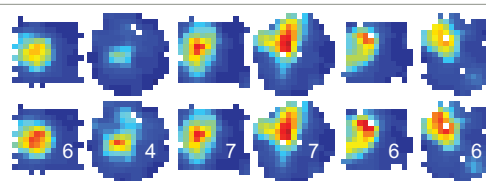
Cell 6



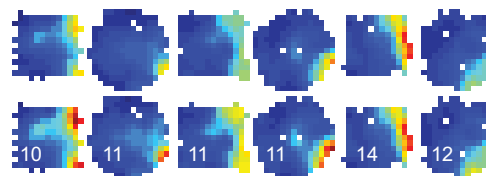
Cell 7



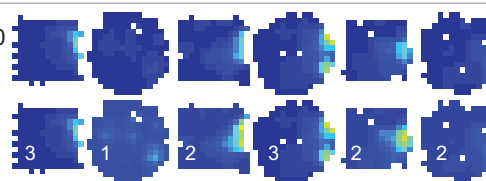
Cell 8



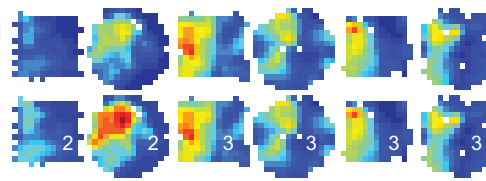
Cell 9



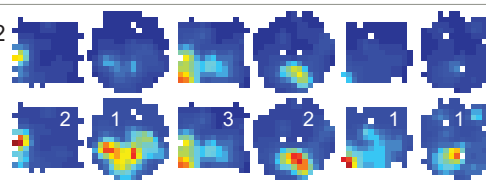
Cell 10



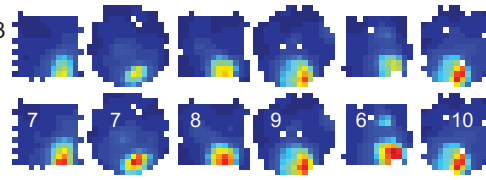
Cell 11



Cell 12

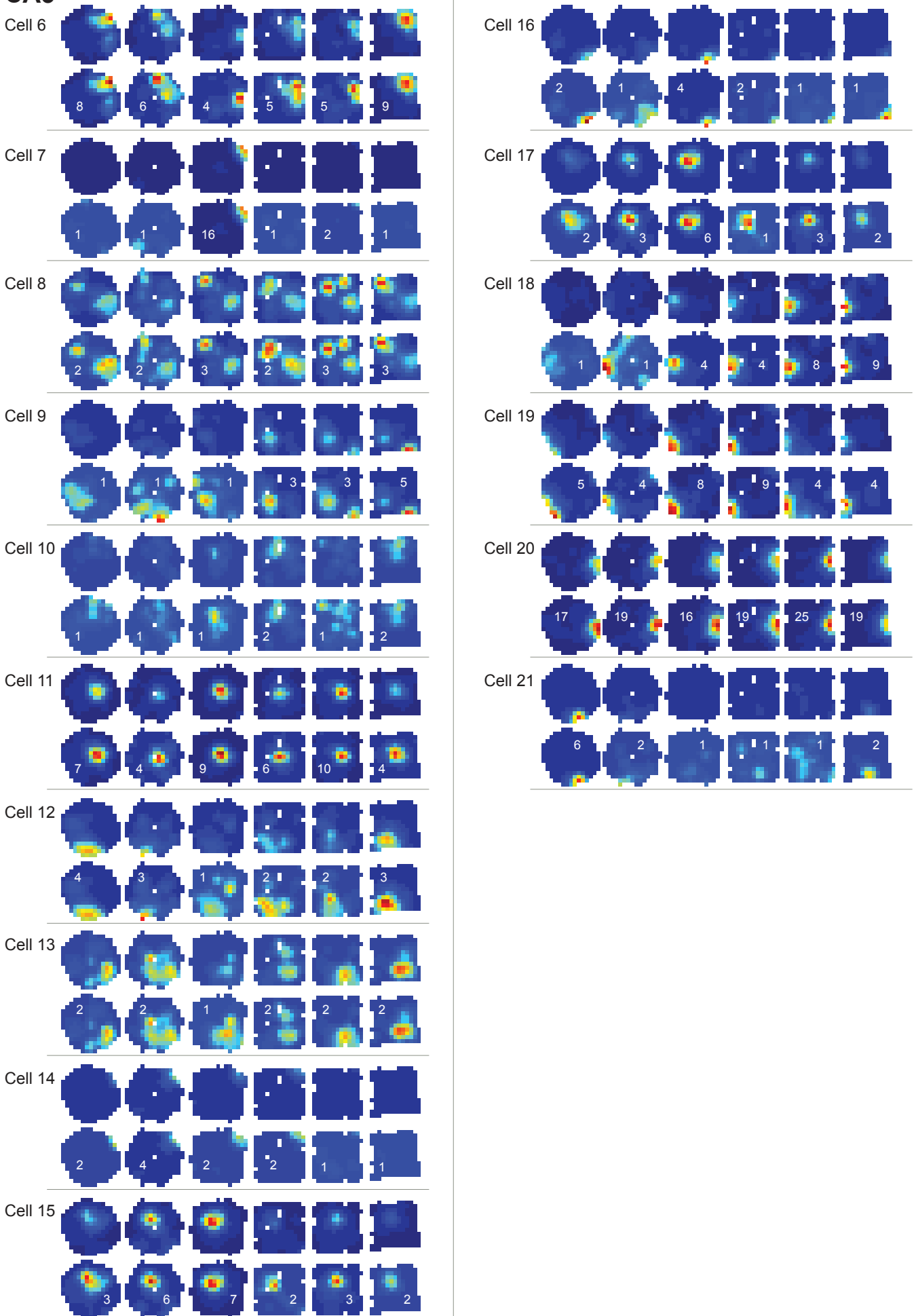


Cell 13



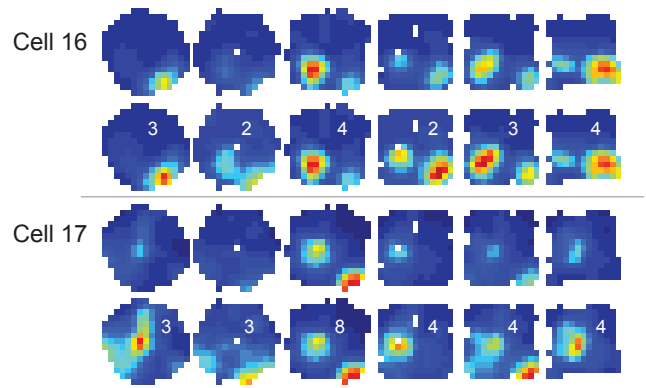
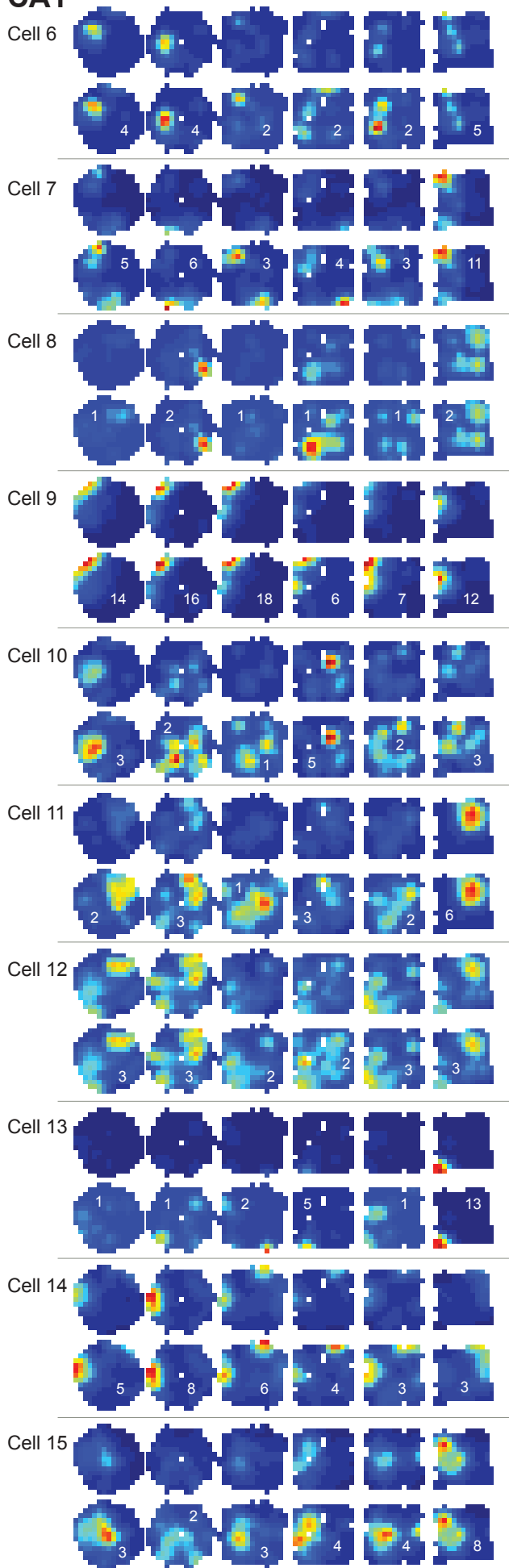
Single location training, Morph day, Rat 3

CA3

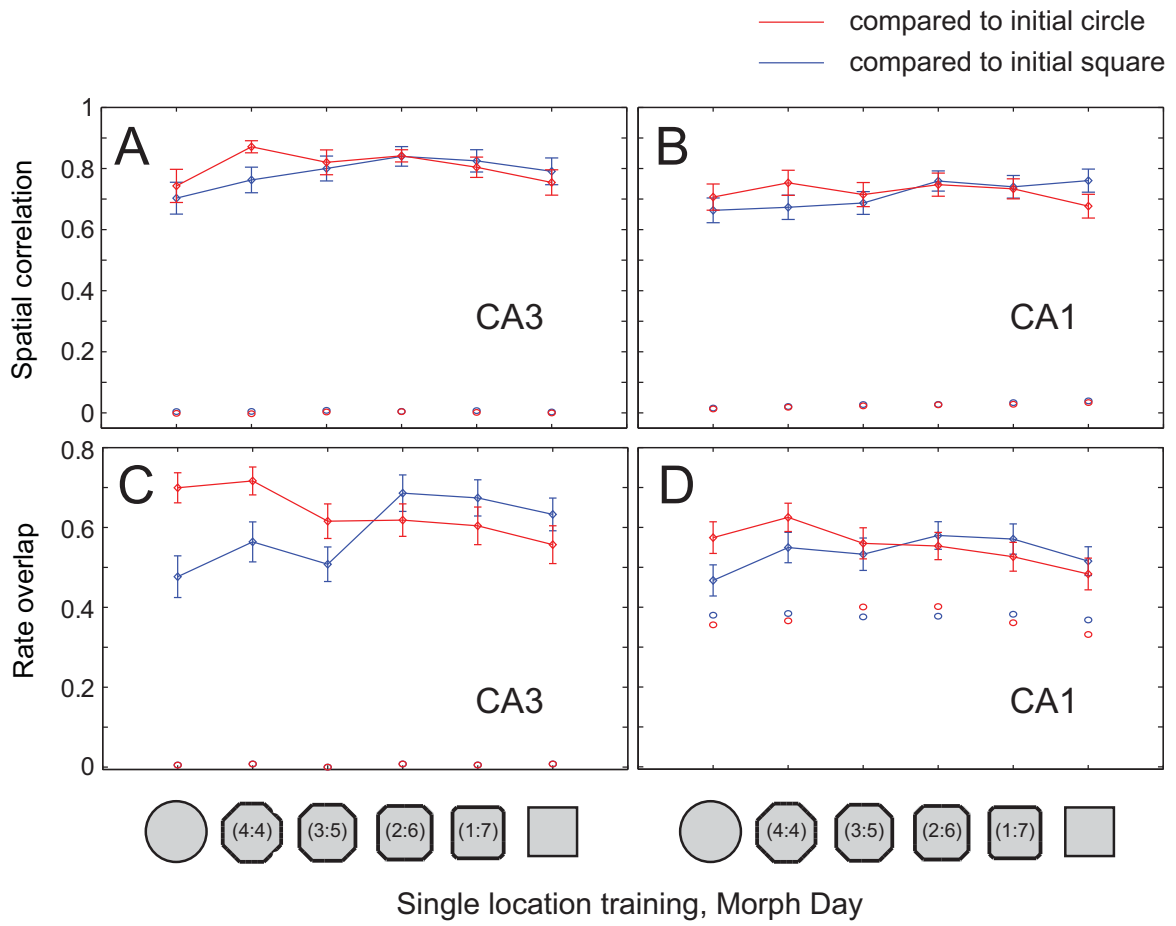


Single location training, Morph day, Rat 3

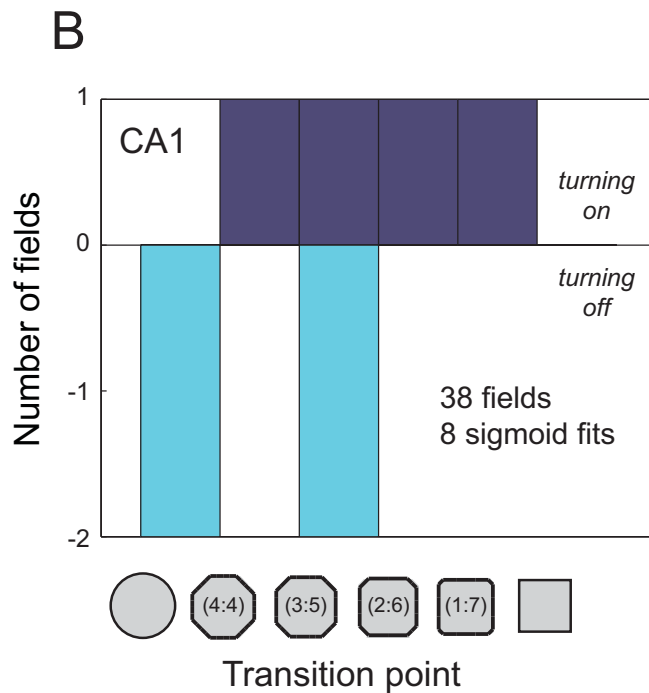
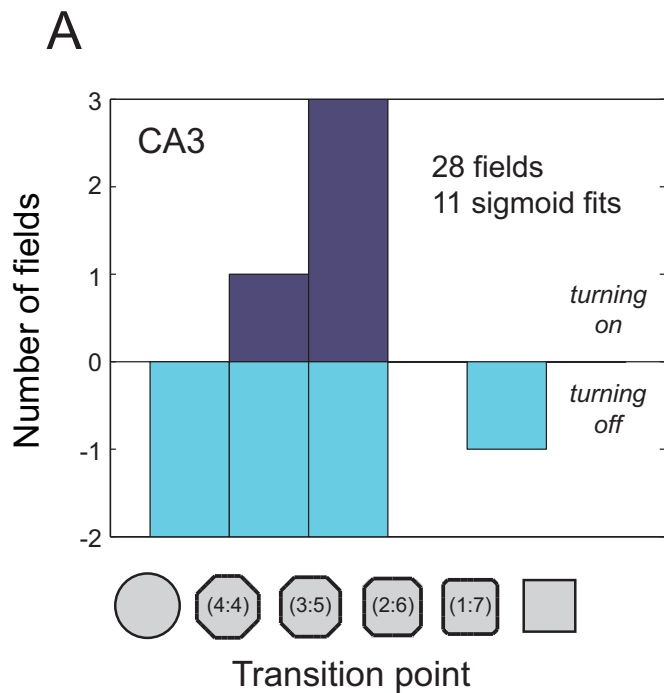
CA1



Supplemental Fig. S3

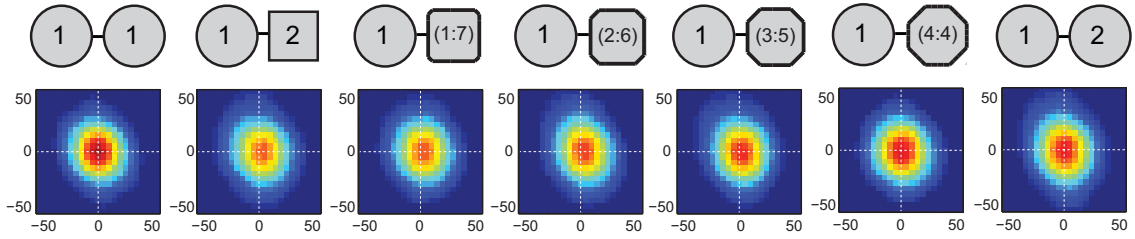


Supplemental Fig. S4



Supplemental Fig. S5

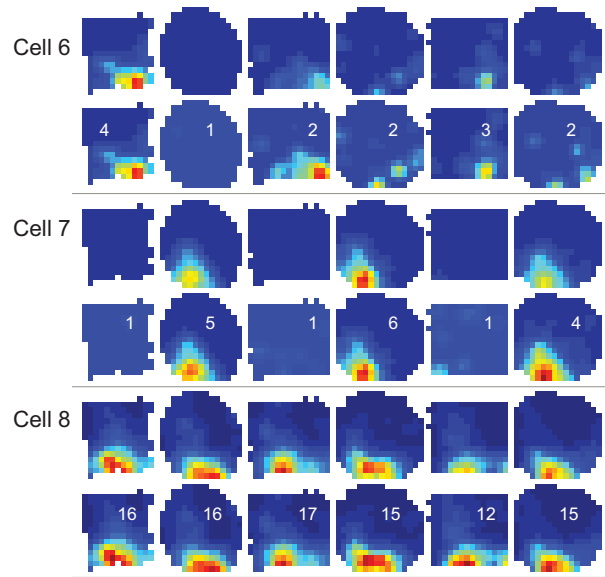
Morph Day, Single location training



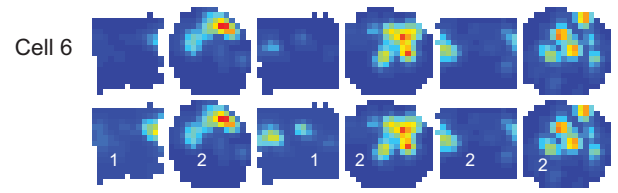
Supplemental Fig. S6

Two location training, Day 4, Rat 6

CA3



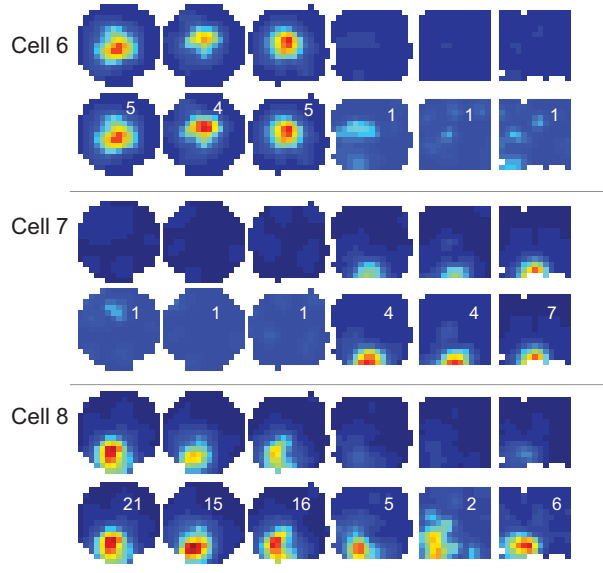
CA1



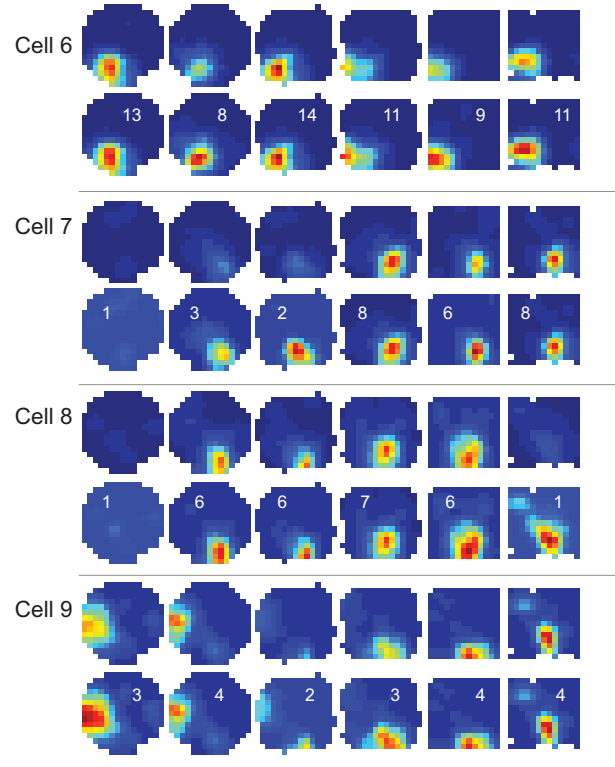
Supplemental Fig. S7

Two location training, Morph Day, Rat 5

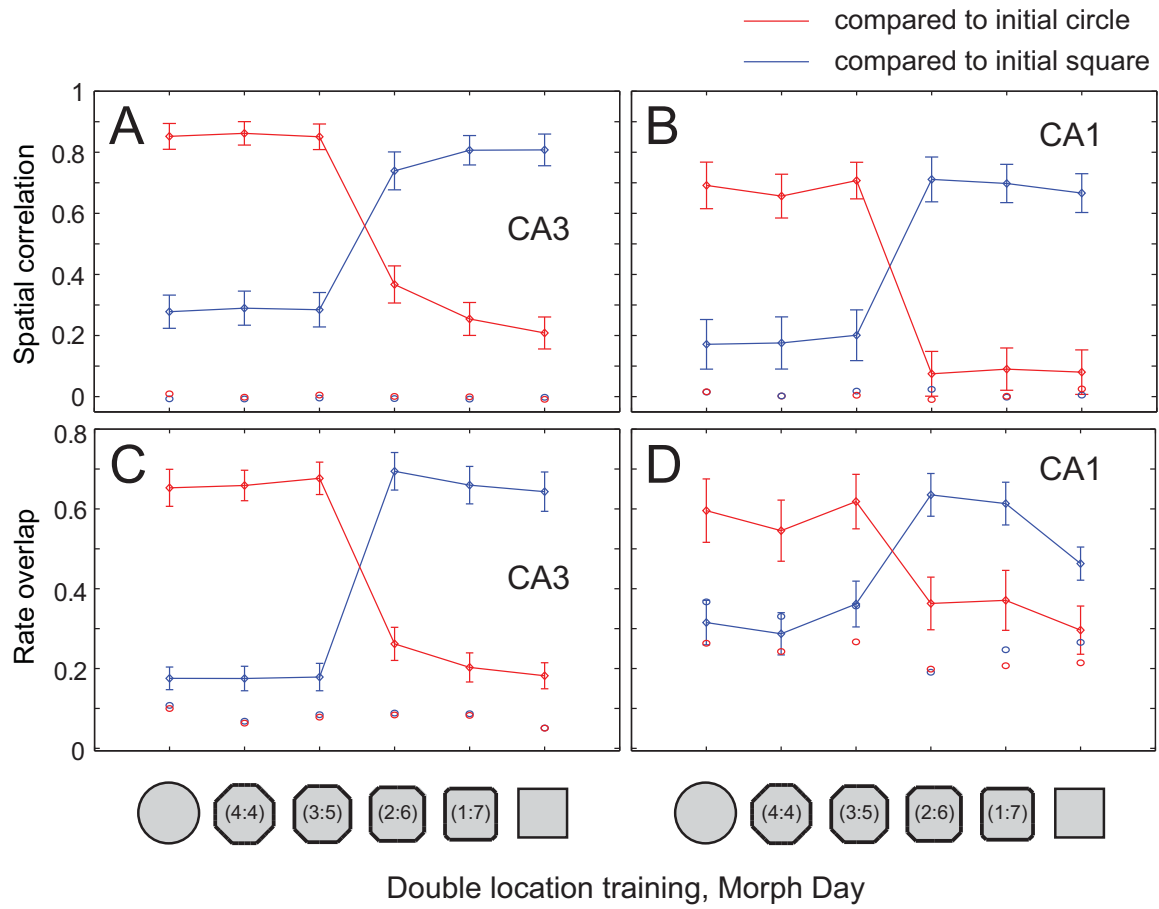
CA3



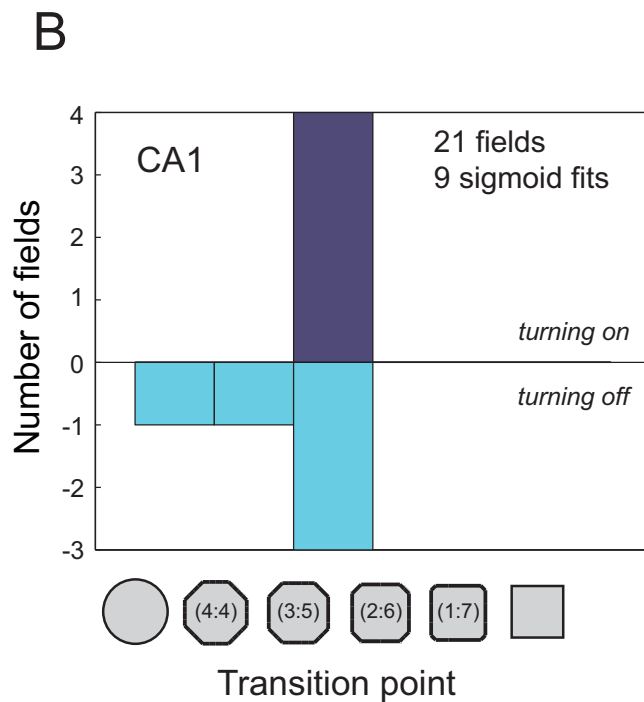
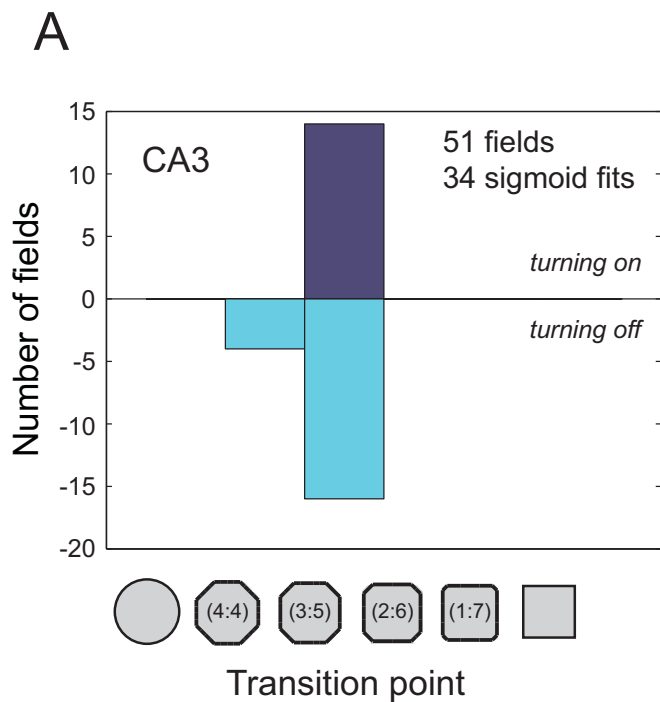
CA1



Supplemental Fig. S8

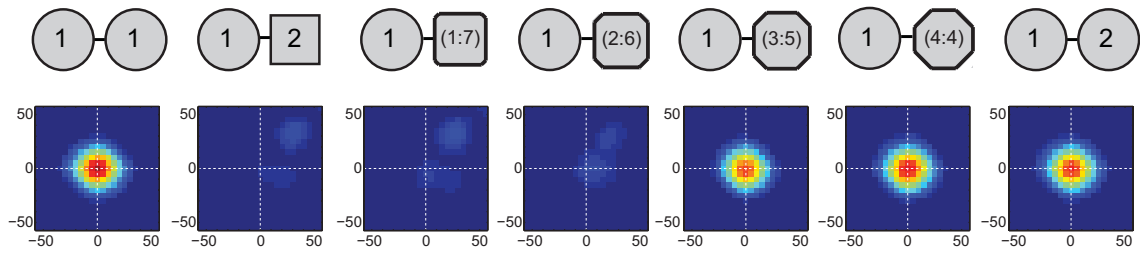


Supplemental Fig. S9



Supplemental Fig. S10

Morph Day, Double location training



















































Supplemental Table S1

Single location training, Day 4

	1 ②	5 6	Statistic ¹	P-value
CA3				
PV correlation	0.32 ± 0.02	0.73 ± 0.02	t(143) = 25.6	P < 0.001
Spatial correlation	0.62 ± 0.06	0.79 ± 0.04	t(30) = 3.2	P < 0.003
Rate overlap	0.25 ± 0.04	0.55 ± 0.05	t(30) = 5.8	P < 0.001
CA1				
PV correlation	0.56 ± 0.01	0.78 ± 0.01	t(143) = 15.4	P < 0.001
Spatial correlation	0.59 ± 0.05	0.75 ± 0.03	t(45) = 2.2	P < 0.03
Rate overlap	0.44 ± 0.04	0.60 ± 0.03	t(40) = 2.7	P < 0.01
1. Two-tailed paired t-test PV: Population vector				

Supplemental Table S2

Single location training, Morph Day

CA3 CA1	PV correlation	Statistic ¹	 	 	 	 	 	 
 	0.67 ± 0.01 0.59 ± 0.02	F(5,715) = 59.2 F(5,715) = 197.3		P < 0.001	P < 0.001	P < 0.001	P < 0.001	P < 0.001
 	0.75 ± 0.01 0.64 ± 0.02		P < 0.001		P < 0.001	P < 0.001	P < 0.001	P < 0.001
 	0.78 ± 0.01 0.62 ± 0.02		P < 0.003	P = 0.7		P < 0.001	P < 0.001	P < 0.001
 	0.88 ± 0.01 0.75 ± 0.01		P < 0.001	P < 0.001	P < 0.001		P = 1.0	P = 1.0
 	0.87 ± 0.01 0.69 ± 0.01		P < 0.001	P < 0.001	P < 0.001	P < 0.001		P = 1.0
 	0.87 ± 0.01 0.67 ± 0.01		P < 0.001	P = 0.7	P < 0.005	P < 0.001	P < 0.03	
	Spatial correlation							
 	0.70 ± 0.05 0.66 ± 0.04	F(5,190) = 2.0 F(5,235) = 4.6		P = 1.0	P = 1.0	P = 0.3	P = 0.3	P = 1.0
 	0.76 ± 0.04 0.67 ± 0.04		P = 1.0		P = 1.0	P = 0.1	P = 1.0	P = 1.0
 	0.80 ± 0.04 0.69 ± 0.04		P = 1.0	P = 1.0		P = 1.0	P = 1.0	P = 1.0
 	0.84 ± 0.03 0.76 ± 0.03		P < 0.02	P < 0.04	P < 0.03		P = 1.0	P = 1.0
 	0.83 ± 0.04 0.74 ± 0.04		P = 0.2	P = 1.0	P < 0.006	P = 1.0		P = 1.0
 	0.79 ± 0.04 0.76 ± 0.04		P < 0.03	P = 1.0	P = 0.3	P = 1.0	P = 1.0	
	Rate overlap							
 	0.48 ± 0.05 0.47 ± 0.04	F(5,155) = 7.2 F(5,235) = 3.6		P = 0.5	P = 1.0	P < 0.02	P < 0.05	P < 0.04
 	0.56 ± 0.05 0.55 ± 0.04		P < 0.04		P = 1.0	P = 0.3	P = 1.0	P = 1.0
 	0.51 ± 0.04 0.53 ± 0.04		P = 0.2	P = 1.0		P < 0.004	P < 0.005	P < 0.004
 	0.69 ± 0.05 0.58 ± 0.03		P < 0.05	P = 1.0	P = 1.0		P = 1.0	P = 1.0
 	0.67 ± 0.05 0.57 ± 0.04		P = 0.1	P = 1.0	P = 1.0	P = 1.0		P = 1.0
 	0.63 ± 0.04 0.52 ± 0.04		P = 1.0	P = 1.0	P = 1.0	P = 0.6	P = 0.3	

1. 1-way repeated measures ANOVA, Bonferroni adjustments for multiple pairwise comparisons

PV: Population vector

















































Supplemental Table S3

Double location training, Day 4

	1 ②	5 6	Statistic ¹	P-value
CA3				
PV correlation	-0.01 ± 0.01	0.05 ± 0.02	t(143) = 4.4	P < 0.001
Spatial correlation	0.09 ± 0.08	0.30 ± 0.08	t(18) = 2.4	P < 0.03
Rate overlap	0.17 ± 0.06	0.20 ± 0.05	t(15) = 0.3	P = 0.8
CA1				
PV correlation	0.44 ± 0.03	0.53 ± 0.03	t(143) = 4.2	P < 0.001
Spatial correlation	0.38 ± 0.09	0.48 ± 0.11	t(15) = 0.6	P = 0.6
Rate overlap	0.44 ± 0.07	0.47 ± 0.07	t(14) = 0.8	P = 0.4
1. Two-tailed paired t-test PV: Population vector				

Supplemental Table S4

Double location training, Morph Day

CA3 \ CA1	PV correlation	Statistic ¹	 	 	 	 	 	 
 	0.03 ± 0.01 0.26 ± 0.03	F(5,715) = 170.7 F(5,715) = 5103.3		P = 0.4	P = 1.0	P < 0.001	P < 0.001	P < 0.001
 	0.02 ± 0.01 0.24 ± 0.02		P = 1.0		P = 0.9	P < 0.001	P < 0.001	P < 0.001
 	0.03 ± 0.01 0.29 ± 0.03		P = 0.1	P < 0.001		P < 0.001	P < 0.001	P < 0.001
 	0.94 ± 0.004 0.76 ± 0.01		P < 0.001	P < 0.001	P < 0.001		P < 0.001	P < 0.001
 	0.86 ± 0.01 0.66 ± 0.02		P < 0.001	P < 0.001	P < 0.001	P < 0.001		P < 0.005
 	0.88 ± 0.01 0.57 ± 0.02		P < 0.001	P < 0.001	P < 0.001	P < 0.001	P < 0.001	
	Spatial correlation							
 	0.28 ± 0.05 0.17 ± 0.08	F(5,150) = 23.1 F(5,100) = 20.4		P = 1.0	P = 1.0	P < 0.001	P < 0.001	P < 0.002
 	0.29 ± 0.06 0.18 ± 0.09		P = 1.0		P = 1.0	P < 0.001	P < 0.001	P < 0.001
 	0.28 ± 0.06 0.20 ± 0.08		P = 1.0	P = 1.0		P < 0.001	P < 0.001	P < 0.001
 	0.74 ± 0.06 0.71 ± 0.07		P < 0.001	P < 0.001	P < 0.001		P = 1.0	P = 1.0
 	0.81 ± 0.05 0.70 ± 0.06		P < 0.001	P < 0.001	P < 0.004	P = 1.0		P = 1.0
 	0.81 ± 0.05 0.67 ± 0.06		P < 0.001	P < 0.001	P < 0.02	P = 1.0	P = 1.0	
	Rate overlap							
 	0.18 ± 0.03 0.32 ± 0.06	F(5,145) = 44.7 F(5,100) = 10.6		P = 1.0	P = 1.0	P < 0.001	P < 0.001	P < 0.001
 	0.18 ± 0.03 0.29 ± 0.05		P = 1.0		P = 1.0	P < 0.001	P < 0.001	P < 0.001
 	0.18 ± 0.03 0.36 ± 0.06		P = 1.0	P = 1.0		P < 0.001	P < 0.001	P < 0.001
 	0.69 ± 0.05 0.64 ± 0.05		P < 0.005	P < 0.001	P < 0.03		P = 1.0	P = 0.8
 	0.66 ± 0.05 0.61 ± 0.05		P < 0.02	P < 0.003	P = 0.07	P = 1.0		P = 1.0
 	0.64 ± 0.05 0.46 ± 0.04		P = 0.7	P = 0.6	P = 1.0	P < 0.03	P = 0.1	

1. 1-way repeated measures ANOVA, Bonferroni adjustments for multiple pairwise comparisons

PV: Population vector